The Planetary Science Journal, 2:98 (10pp), 2021 June https://doi.org/10.3847/PSJ/abde4b

The Main Asteroid Belt: The Primary Source of Debris on Comet-like Orbits

P. M. Shober, E. K. Sansom, P. A. Bland, H. A. R. Devillepoix, M. C. Towner, M. Cupák, R. M. Howie, B. A. D. Hartig, and S. L. Anderson
Space Science & Technology Centre, School of Earth and Planetary Sciences, Curtin University, GPO Box U1987, Perth, WA 6845, Australia
patrick.shober@postgrad.curtin.edu.au
Received 2020 December 12; revised 2021 January 17; accepted 2021 January 19; published 2021 May 13

Abstract

Jupiter-family comets (JFCs) contribute a significant amount of debris to near-Earth space. However, telescopic observations of these objects seem to suggest that they have short physical lifetimes. If this is true, the material generated will also be short-lived, but fireball observation networks still detect material on cometary orbits. This study examines centimeter-to-meter-scale sporadic meteoroids detected by the Desert Fireball Network from 2014 to 2020 originating from JFC-like orbits. Analyzing each event's dynamic history and physical characteristics, we confidently determined whether they originated from the main asteroid belt or the trans-Neptunian region. Our results indicate that <4% of sporadic meteoroids on JFC-like orbits are genetically cometary. This observation is statistically significant and shows that cometary material is too friable to survive in near-Earth space. Even when considering shower contributions, meteoroids on JFC-like orbits are primarily from the main belt. Thus, the presence of genuine cometary meteorites in terrestrial collections is highly unlikely.

Unified Astronomy Thesaurus concepts: Meteoroids (1040); Solar system (1528); Meteorites (1038); Fireballs (538); Meteors (1041); Short period comets (1452); Near-Earth objects (1092); Small Solar System bodies (1469); Meteorite composition (1037); Orbital evolution (1178); Dynamical evolution (421); Orbits (1184)

1. Introduction

Jupiter-family comets (JFCs) are short-period comets near the ecliptic plane that are strongly influenced by Jupiter. They originate from the outer solar system in the scattered disk (Duncan & Levison 1997) and are comprised of primitive volatile-rich material. They are conventionally defined by their Tisserand's parameter ($2 < T_J < 3$), which is an approximately conserved value in the circular restricted three-body problem (object—Jupiter–Sun). This is a better way to classify the orbits of small planetary bodies compared to the traditionally used orbital periods (Levison & Duncan 1994). The physical properties of JFCs have been explored in numerous studies based on meteor/fireball analysis (Jenniskens 2006; Borovička et al. 2007; Madiedo et al. 2014), telescopic observations (Fernández et al. 2005, 2013), dynamical modeling (Duncan et al. 2004; Di Sisto et al. 2009; Nesvorný et al. 2010; Tancredi 2014), and space missions (Brownlee et al. 2004; A'Hearn et al. 2005; Sunshine et al. 2006; Fornasier et al. 2015). Each method provides information about different size ranges of objects on JFC-like orbits.

When observing meteors streak across the night sky, we are typically witnessing the size range of the smallest objects in the near-Earth space (dust-sized; $\ll 10^{-3}$ kg). Conversely, telescopic observations are instrumental in characterizing the most massive objects (hundreds of meters to kilometers in diameter). This gap between the meteor and telescopic observations is the primary range for the progenitors of meteorites. Usually spanning centimeters to meters in scale, this size range has been interpreted from fireballs and the meteorites they produce on the ground (Borovička et al. 2015; Granvik & Brown 2018).

Based on telescopic observations and dynamical studies, many researchers believe there is a paucity of JFCs at subkilometer scales (Meech et al. 2004; Fernández & Morbidelli 2006; Nesvorný et al. 2017). This lack of objects at smaller sizes is thought to be related to the inferred brief physical lifetimes (10^3–10^4 yr) of JFCs in the inner solar system (Levison & Duncan 1997; Fernández et al. 2002; Di Sisto et al. 2009). Due to their low bulk density and high volatile content, JFCs should fade away relatively quickly when within ~3 au.

Nevertheless, despite the predicted subkilometer paucity, fireball observation networks have many accounts of durable centimeter-to-meter-sized meteoroids originating from JFC-like orbits (Brown et al. 2000; Borovička et al. 2013; Spurný et al. 2017; Borovička et al. 2019). By examining meter-sized terrestrial impactors, it was found that about 5%–10% had JFC-like orbits, relatively consistent with the flux estimates based on larger kilometer-scale near-Earth objects (NEOs; Brown et al. 2016). Yet they found that only half of these displayed weaker-than-average structures based on their atmospheric ablation characteristics. Two of the five JFC-like events discussed were calibrated meteorite falls (Maribo and Sutter's Mill) likely to be from the main asteroid belt. Meanwhile, the remaining three events all came from US Government sensor (USG) data; two of these had a semimajor axis of ~2.9 au, i.e., well within the bounds of the outer main belt. Also, it has since been demonstrated that the orbital information collected by USG events is generally unreliable (Devillepoix et al. 2019).

Additionally, another study recalculated the orbits for 25 meteorite falls and identified their likely source regions using an advanced NEO model (Granvik & Brown 2018; Granvik et al. 2018). The only meteorite that had a mean JFC probability ⩾50% was an H5/6 ordinary chondrite, Ejby. Furthermore, the fall with the second-highest JFC source region probability was another H5, Košice. However, both of these falls have relatively significant initial velocity uncertainties,

increasing the uncertainty for the source region analysis. Carbonaceous chondrites Maribo and Sutter's Mill (both CM2) also had probabilities of coming from the JFCs above 20%. Nevertheless, no precisely observed meteorite falls have yet come from an unambiguously cometary orbit.

The Taurid complex has also been discussed as being capable of larger, possibly meteorite-dropping, meteoroids (Brown et al. 2013). These meteoroids can be hundreds of kilograms in size, an order of magnitude higher than other showers. However, other studies have found that while the Taurids can produce very large meteoroids, they are still very weak and unlikely to produce meteorites (Borovička et al. 2017). Given the highly evolved orbit of comet 2P/Encke and the other noncometary possible parent bodies in similar orbits, this subset of observed Taurids also does not likely reflect the vast majority of JFC meteoroids (Asher et al. 1993).

Based on debiased NEO orbital and absolute-magnitude distributions, it is expected that the contribution from the JFC region is a few percent, on average (Bottke et al. 2002; Granvik et al. 2018). The contribution seems to increase at smaller sizes, reaching ∼10% of the NEO population below diameters of 100 m (Granvik et al. 2018). However, this estimate assumes that JFCs are more likely to become dormant than disintegrate, as JFC disruptions are less commonly observed compared to long-period comets. If this assumption breaks down at smaller sizes, then the JFC contribution to the NEO meteoroid flux may be negligible.

If the hypothesis that the physical lifetimes of subkilometer comets are very short is accurate, why do fireball networks still observe centimeter–meter debris originating from comet-like orbits? Does the larger cometary debris we observe impacting the Earth originate from comets?

The massive orbital data set collected by the Desert Fireball Network (DFN) was utilized to answer these questions. The DFN is the largest single photographic fireball network in the world, covering over 2.5 million km^2 of Australia. This massive project is part of a worldwide collaboration, the Global Fireball Observatory (GFO; https://gfo.rocks/), currently consisting of 18 partner institutions (Devillepoix et al. 2020). The GFO has a semiautomated data processing pipeline that sorts images, detects fireball events, and triangulates these events (Howie et al. 2017; Jansen-Sturgeon et al. 2019; Sansom et al. 2019a, 2019b; Towner et al. 2020).

2. Materials and Methods

2.1. Experimental Design

The data set used for this study was collected by the DFN. Covering over one-third of the Australian outback, the DFN is the largest photographic fireball network globally. The observations made by the DFN are invaluable and provide key insights into the debris impacting the Earth daily.

When parsing through the data set for this study, all events that originated from an orbit with a JFC-like Tisserand's parameter ($2 < T_J < 3$) and had a significant initial mass ($\geqslant$0.01 kg) were gathered. The Tisserand's parameter is an approximately conserved value in the three-body problem and is regularly used to distinguish between different kinds of small planetary bodies (Levison & Duncan 1994). Typically, this three-body problem includes the Sun, Jupiter, and the asteroid or comet; since Jupiter is seen as the primary perturber, the parameter is written as T_J.

2.1.1. Trajectory Analysis and Orbit Determination

The fireball events detected by the DFN have atmospheric trajectories fitted using a modified straight-line least-squares (SLLS) and an extended Kalman smoother for the velocity profile (Sansom et al. 2015). The uncertainties associated with the fitted fireball trajectories are propagated from the residuals of the fit itself, along with the timing and positional uncertainties of the events' observations. The observational uncertainties are handled and incorporated by the Kalman filter. The initial masses and corresponding uncertainties were also determined using a dynamic model in a reverse extended Kalman filter (Sansom et al. 2015). The preatmospheric orbits are then determined numerically including any relevant perturbations by integrating the meteoroid's state until it was outside the Earth's sphere of influence (Jansen-Sturgeon et al. 2019). The orbital uncertainties are then obtained with a Monte Carlo approach by numerically integrating samples randomly drawn from within the initial state uncertainties at the top of the atmosphere.

2.1.2. Addressing Observational Biases

The DFN uses photographic observations of fireballs to help better understand the debris in the inner solar system. However, to obtain meaningful results from this data set, we must first address any observational biases.

The first bias we address is that the DFN is optimized for meteorite-dropping fireball events (∼0.5 limiting magnitude; Howie et al. 2017). In this study, we limit the meteoroids considered to a minimum initial mass of 10 g. This bias does not affect the results, as both asteroidal and cometary populations are known to produce material within this size range (Boehnhardt 2004; Fernández 2009).

Second, we must ensure that the DFN observations are not biased against observing either asteroidal or cometary debris due to the orbits in which they exist. The primary bias to be concerned with is due to gravitational focusing. Since meteoroids with a lower relative velocity are more gravitationally focused, the terrestrial impact population contains a larger proportion of asteroidal impactors from orbits with smaller semimajor axis values. However, this study is concerned with meteoroids originating from similar orbits; thus, they are all weighted nearly equally. Other observational biases are associated with photographic fireball observations; however, none of these would have any affect on the results of this study. For a more exhaustive list and discussion of DFN observational biases, please reference Shober et al. (2020a).

2.1.3. Data Selection

In a manual check of all of the fireball observations and triangulations, any events with poor data were removed (e.g., the fireball was very far from the cameras, the convergence angles for triangulations were too small, etc.). The orbital uncertainties of the meteoroids must be sufficiently low to obtain meaningful statistics from the Monte Carlo numerical integrations. If the uncertainties are too large, the number of samples required to get statistically reasonable results may be computationally unfeasible. Additionally, meteoroids with T_J values within three standard deviations of $T_J = 3.0$ or 2.0 were excluded to remove ambiguous events.

In this study, only fireballs with no shower associations were considered, i.e., sporadic. Therefore, any events with distinctly

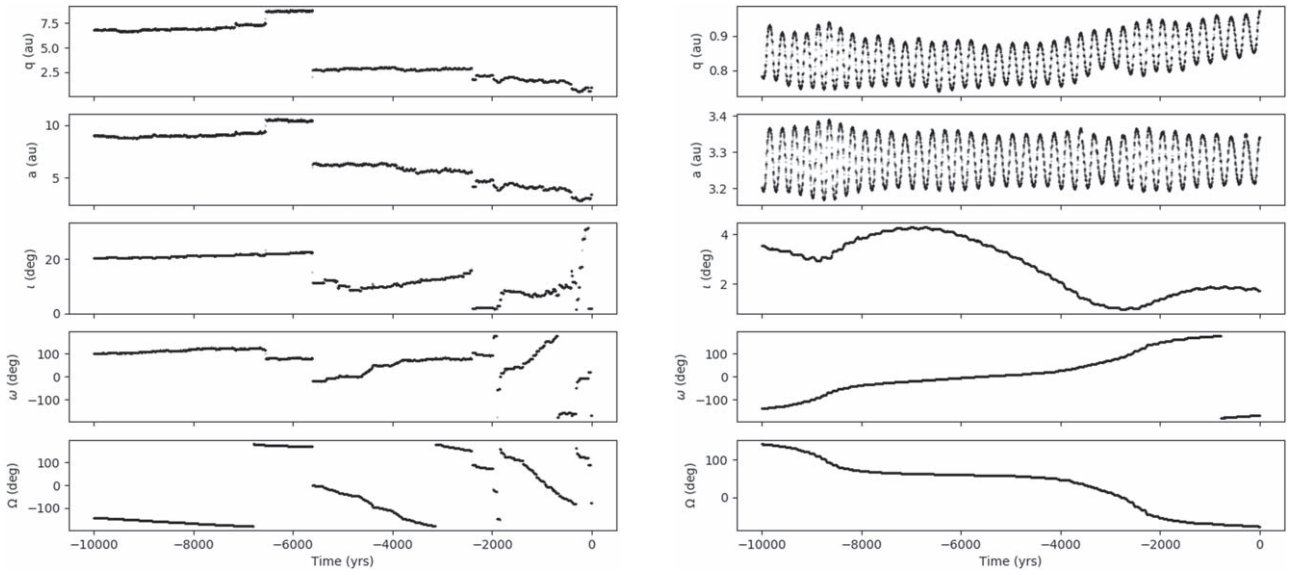

Figure 1. Backward integrations over −10 kyr of two particles generated within the triangulated trajectory uncertainties of event DN200104_01 where q is the perihelion, a is the semimajor axis, ι is the inclination, ω is the argument of perihelion, and Ω is the longitude of the ascending node. On the left, we show a particle on a chaotic unstable orbit typical of a comet with numerous Jupiter close encounters. On the right, another particle provides an example of a stable orbit following a predictable path with no close encounters with Jupiter. This specific fireball event lasted over 5 s and was recorded by four DFN stations, providing an excellent trajectory fit with very minimal uncertainties. Thus, this demonstrates the difficulty associated with backward propagation of meteoroids coming from orbits on the edge of two source regions (JFC and main belt, in this case).

cometary physical and dynamical characteristics could indicate a process to preserve cometary material in this range for longer periods. Using primarily the D_J similarity criterion, we sorted through associations with a limiting value of $D_J < 0.15$ (Jopek 1993). A more inclusive limiting value was used to eliminate any potential shower events. We verified associations from this subset by comparing orbital elements, shower dates, right ascensions and declinations, initial velocities, nodal directions, and arguments of perihelion, along with other similarity criteria (Southworth & Hawkins 1963; Drummond 1981). The meteor shower data used were taken from all showers listed by the IAU Meteor Data Center,[1] with a higher weight placed on established showers.

The fireball data used within this study, including uncertainties, are available at 10.5281/zenodo.4710556.

We characterized the physical and dynamical characteristics of the sporadic meteoroids on JFC-like orbits using fireball data from the DFN with the following goals:

1. determining the proportion of genetically cometary material in excess of 10 g on sporadic JFC-like orbits,
2. assessing whether or not the physical lifetimes of JFC meteoroids in the meteorite-dropping size range are shorter than the disassociation lifetimes of cometary streams, and
3. finding out if it is possible to get a meteorite from a JFC-orbit and what it would look like.

2.2. Dynamic Analysis

As shown in previous studies, genuine JFCs originating from the outer solar system tend to move on chaotic orbits over thousands of years, encountering Jupiter frequently over their lifetime (Tancredi 1995; Levison & Duncan 1997). In this work, we have adopted a similar search strategy to past studies by numerically integrating the fireball trajectories backward 10 kyr and identifying fireballs originating from "stable" and "unstable" orbits (Fernández & Sosa 2015; Fernández et al. 2014; Tancredi 2014). For each event, a Monte Carlo simulation was undertaken where 10 simulations with 100 particles were integrated over −10 kyr. These simulations were conducted using the IAS15 integrator, taking into account all planetary perturbations and close encounters considering all of the planets and the Moon (Rein & Liu 2012; Rein & Spiegel 2015). The particles were initialized within the formal triangulation uncertainties assuming a Gaussian distribution. The particles' histories were then each assessed and labeled as either "stable" or "unstable" over the previous 10 kyr. Those with frequent unpredictable jumps in their orbital elements were considered unstable (Figure 1(a)), whereas those in resonances and following smooth trajectories with little change in perihelion distance were considered stable (Figure 1(b)). The final instability probabilities and associated uncertainties were then obtained by taking the mean and standard deviation of the sample means.

2.3. Physical Analysis

In order to characterize the physical properties, we determined the PE value for each fireball. The PE criterion was first introduced as a way to discriminate between different meteoroid compositions based on the ability to penetrate the atmosphere (Ceplecha & McCrosky 1976). It has since been used in numerous studies to assess the physical nature of impacting meteoroids (Ceplecha 1994; Brown et al. 2013, 2016; Borovička et al. 2015).

[1] https://www.ta3.sk/IAUC22DB/MDC2007/

Table 1
Traditional PE Classifications Based on the Atmospheric Density at Terminal Height (Ceplecha & McCrosky 1976)

Type I	$PE > -4.60$	Ordinary chondrite-like
Type II	$-5.25 < PE \leqslant -4.60$	Carbonaceous chondrite
Type IIIa	$-5.70 < PE \leqslant -5.25$	Short-period cometary
Type IIIb	$PE \leqslant -5.70$	Weak cometary material

The PE value is given by

$$PE = \log(\rho_E) - 0.42\log(m_\infty) + 1.49\log(V_\infty) - 1.29\log(\cos Z_R), \quad (1)$$

where ρ_E is the density of the atmosphere at the end of the luminous trajectory (and the reason for the acronym "PE"), m_∞ is the initial mass of the meteoroid in grams, V_∞ is the initial velocity of the meteoroid in kilometers per second, and Z_R is the local entry angle measured from the zenith.

The PE values are divided into four types: ordinary chondrite-like (type I), carbonaceous (type II), short-period cometary (type IIIa), and weak cometary (type IIIb; Ceplecha et al. 1998). The boundaries for these groups are denoted in Table 1. The PE criterion is an extremely useful metric to evaluate the physical properties of meteoroids; however, the types are not strictly correct. While providing generally accurate results of relative strength, the physical composition of any individual meteoroid is uncertain due to the other factors that affect the durability while transiting the atmosphere (e.g., macro-scale fractures; Popova et al. 2011; Borovička et al. 2020).

We additionally computed the ballistic coefficient (α) and mass-loss parameter (β) based on the fireball observations (Gritsevich & Stulov 2006; Gritsevich 2007; Lyytinen & Gritsevich 2016). Using these parameters, one can quickly identify potential meteorite-dropping events (Sansom et al. 2019a). They can be calculated for any event showing some level of deceleration by using the velocity and height data (https://github.com/desertfireballnetwork/alpha_beta_modules).

In Figure 4, we determined potential meteorite-dropping fireballs using the α–β values. Assuming that a 50 g final mass is the minimum meteorite-dropping mass, the meteorite-dropping lines were calculated with the following equations:

$$\ln\beta = \ln[13.2 - 3\ln(\alpha\sin\gamma)], \quad \mu = 0, \quad (2)$$

$$\ln\beta = \ln[4.4 - \ln(\alpha\sin\gamma)], \quad \mu = \frac{2}{3}, \quad (3)$$

when assuming $\rho_m = 3500\,\mathrm{kg\,m^{-3}}$ (meteoroid density) and $c_d A = 1.5$ (product of drag coefficient and initial shape coefficient). Considering that the contribution from the outer main belt may be significant, where many objects have low albedos (DeMeo & Carry 2014; DeMeo et al. 2015; Takir et al. 2015; e.g., C and D types), we also plotted the equivalent lines for a CM-like density (Consolmagno et al. 2008; $\rho_m = 2240\,\mathrm{kg\,m^{-3}}$) using the following equations:

$$\ln\beta = \ln[14.09 - 3\ln(\alpha\sin\gamma)], \quad \mu = 0, \quad (4)$$

$$\ln\beta = \ln[4.7 - \ln(\alpha\sin\gamma)], \quad \mu = \frac{2}{3}. \quad (5)$$

Together, the dynamic simulations and analysis of the material properties can better elucidate what types of material regularly impact the Earth from JFC-like orbits in the considered size range.

2.4. Statistical Analysis

Based on the dynamical and physical analysis, the source populations can be inferred for each meteoroid in this study. However, given the sample size, what does this tell us about the entire population of small JFC-like meteoroids?

In order to answer this question, we utilize a Markov Chain Monte Carlo to sample from the posterior probability distribution. The Bayesian model was created with the Python PyMC3 probabilistic programming package using the No-UTurn Sampler (Salvatier et al. 2016). A beta distribution was used as a prior with the hyperparameters (α) based on a study that examined the dynamical characteristics of 58 near-Earth JFCs ($q < 1.3$ au; Fernández & Sosa 2015). This corresponded to the hyperparameters $\alpha = [1.38, 8.62]$ and an observation vector $c = [48, 2]$; the hyperparameters were weighted less, as they were based on kilometer-scale objects. Additionally, as a comparison, an uninformed uniform prior of $\alpha = [1.0, 1.0]$ was included. In total, 15,000 samples from the posterior were taken to estimate the posterior. To be counted as genetically JFC in origin in the model, the meteoroids would need to have a >50% probability of originating from an unstable orbit and be of PE types II or III. We considered a PE type II as plausibly cometary due to previous arguments that meteorites from JFCs could possibly be represented by primitive carbonaceous chondrites (Gounelle et al. 2008).

3. Results

In this study, we examined fireballs not associated with meteor showers detected by the DFN during 4 yr of observations. All of the fireballs considered were generated by meteoroids that originated from JFC-like orbits ($2 < T_J < 3$). The source region of these meteoroids, the main belt or JFCs, was determined by analyzing the orbital stability and physical durability during atmospheric transit. It takes only ~1000 yr to become orbitally disassociated from a JFC shower. Therefore, the identification of sporadic JFC material would indicate a minimum physical lifetime equal to the disassociation time (Tancredi 1995). However, a lack of sporadic cometary debris in fireball observations would be clear evidence that the physical lifetimes are less than 1000 yr.

3.1. Orbital Characteristics of Sporadic JFC-like Meteoroids

The JFCs move on chaotic orbits compared to main-belt asteroids, on the order of thousands of years (Tancredi 1995). During their lifetimes, their orbital evolution is controlled by the numerous close encounters they have with Jupiter. Of the 50 sporadic JFC-like fireball events analyzed in this study, nearly all of the meteoroids come from stable orbits over the previous 10 kyr (see https://doi.org/10.5281/zenodo.4710556). This is inconsistent with the dynamics diagnostic of JFCs.

Only three events have a high probability of originating from an unstable orbit. However, one of these comes from within 3 au and crosses one of the major mean-motion resonances (MMRs). Events DN150817_01 and DN161028_02 have the highest probability of originating from unstable cometary orbits, with $86.1\% \pm 5.5\%$ and $90.8\% \pm 3.0\%$ of the particles integrated being chaotic, respectively. As seen in Figure 2, event DN150816_04 overlaps the 7:3 MMR when considering

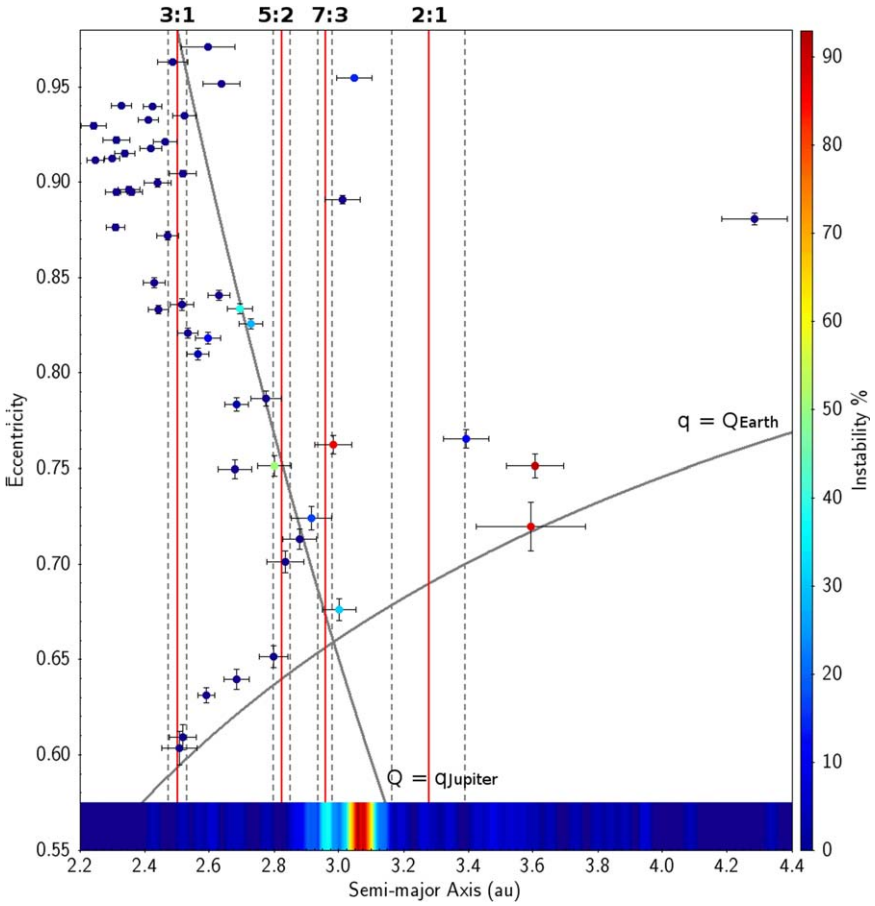

Figure 2. Triangulated semimajor axis vs. eccentricity for 50 nonshower JFC-like fireballs observed by the DFN that have predicted initial masses greater than 10 g. Error bars denote the formal 1σ orbital uncertainties associated with each meteoroid, and coloration is indicative of the orbital stability determined through numerical integrations of -10 kyr. The vertical red lines indicate the major MMRs, with the dashed gray lines marking the maximum libration in semimajor axis (Tancredi 2014). Most of the events originate from stable orbits near the MMRs. The densogram (http://www.star.bris.ac.uk/mbt/stilts/sun256/layer-densogram.html) at the bottom of the plot represents the semimajor axis density for all near-Earth ($q < 1.3$ au) JFCs according to the NASA HORIZONS system (http://ssd.jpl.nasa.gov/horizons.cgi).

triangulation uncertainties, whereas events DN150817_01 and DN161028_02 both lie outside the normal range of the main belt with a semimajor axis of ∼3.6 au. Several meteoroids have inconclusive dynamical histories; these include six events where several of the particles integrated evolved chaotically over thousands of years. On the other hand, nearly all of these inconclusive events come from orbits near MMRs, thus indicating that orbital uncertainty is very likely the cause of the inconclusive results. Otherwise, >80% of the events originate from extremely stable orbits near one of the primary MMRs (Figure 2).

A large majority of the fireballs examined in this study do not fall within the range consistent with observed kilometer-scale JFCs. As seen in Figure 2, a majority of the near-Earth JFCs exist near ∼3.1 au, where only a handful of events originate. However, only one of the four events in this range comes from an unstable orbit. This is in line with a previous model, where they found that main-belt material can contaminate the JFC population but would primarily be contained to the original bounds of the main belt (Hsieh & Haghighipour 2016). However, four of the 50 events examined fall beyond the 2:1 MMR, and of these, only two have higher probabilities of originating from unstable orbits (Figure 2). Additionally, the inclinations of the fireballs examined tend to be relatively diffuse, but are most concentrated toward low values within the 0°–25° range. This is more reconcilable with the main-belt inclination distribution than the JFC distribution, which is more highly concentrated around ∼12° (see https://doi.org/10.5281/zenodo.4710556).

3.2. Physical Characteristics of Sporadic JFC-like Meteoroids

The PE criterion characterizes the composition of meteoroids based on their ability to penetrate the atmosphere (Ceplecha & McCrosky 1976). This metric is empirically determined based on the terminal height of the fireball, the entry mass, the velocity at the top of the atmosphere, and the impact angle. The PE criterion has been used for decades to understand the physical properties of meteoroids based on their atmospheric ablation characteristics (Borovička et al. 2015; Brown et al. 2016). The values are traditionally split accordingly (Ceplecha et al. 1998).

The use of the PE criterion can be quite valuable when analyzing many fireballs; however, the types are not strictly exclusive and should not be taken as absolute truth. Other properties beyond physical composition can blur the lines between the types, such as macro-scale cracks (Popova et al. 2011; Borovička et al. 2020). As expected, considering the dynamic analysis, many of the JFC-like fireballs in this study are quite durable and strong (Figure 3). We only see meteoroids of types I or II; i.e., none fall into the standard categories

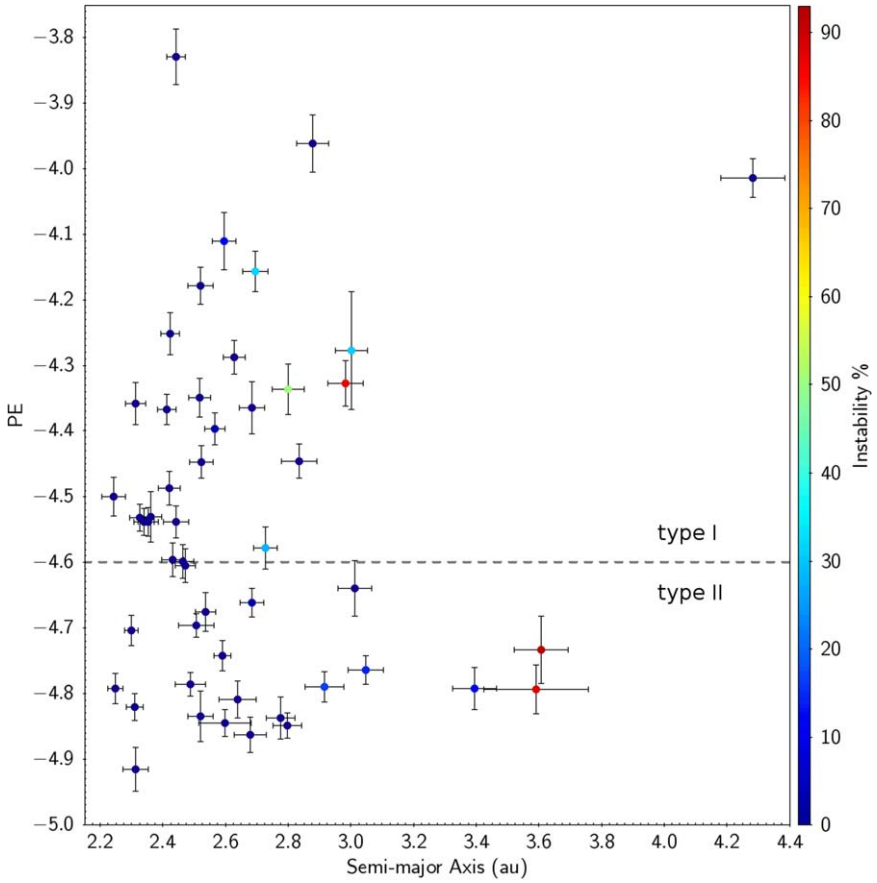

Figure 3. Sporadic JFC-like fireballs observed by the DFN with a minimum initial mass of 10 g. The end heights of meteors can be used to ascertain the physical nature of meteoroids using the PE criterion (Ceplecha & McCrosky 1976). The PE values for the 50 fireballs examined are overwhelmingly stronger than the traditional comet types (types IIIa and IIIb). The error bars associated with each meteoroid's semimajor axis and PE value are due to triangulation uncertainties.

associated with cometary material. Out of the 50 fireballs, 28 would be classified as type I and 22 as type II. Some short-period showers actually can produce more durable debris with similar strengths (Brown et al. 2013). Therefore, the PE criterion alone is not a sure way to distinguish between different materials for an individual fireball. In general, the PE types can give a sense of how strong the initial meteoroid was, but when combined with the dynamic analysis, the source population of a meteoroid can be more confidently obtained (main belt or JFC).

3.2.1. Meteorite Production from JFC-like Meteoroids

Traditionally, the empirical criteria to predict whether a fireball has produced a meteorite on the ground (a "fall") are height and velocity below 35 km and 10 km s^{-1}, respectively, at the end of the luminous portion of the atmospheric trajectory (Wetherill & ReVelle 1981). This gives us an easy way to identify possible recoverable falls quickly. A more rigorous way to determine which fireballs result in meteorites has since been demonstrated, where the ballistic coefficient (α) and the mass-loss parameter (β) are fit to the fireball observations (Sansom et al. 2019a).

In Figure 4, we see that several of the JFC-like fireballs examined in this study are quite durable. At least some events are likely to have meteorites on the ground that are >50 g (DN150905_01 and DN191020_02). However, these events are likely asteroidal in origin based on their dynamic stability over the previous 10 kyr and their PE classification. No events with high instabilities over the previous 10 kyr or of type II drop meteorites in this study. Thus, meteorites from JFC-like orbits do occur, but they are all representative of main-belt material.

4. Discussion

Based on a dynamical and physical analysis of sporadic JFC-like ($2 < T_J < 3$) fireballs with initial masses >10 g, we find a clear abundance of stronger, dynamically stable meteoroids (Figure 3). As seen in Figure 2, most meteoroids evolve in a deterministic way over the previous 10 kyr and have proximity to major MMRs. Dynamic instability is a diagnostic feature of JFCs originating from the outer solar system, as they suffer frequent close encounters with Jupiter (Tancredi 1995, 2014). The predictable evolution of nearly all of the meteoroids in this study is therefore indicative of their likely origin in the main belt. Additionally, events with indeterminate histories, where a nonnegligible subset of particles evolved chaotically, also mostly lie near the primary MMRs, as does one of the three events with >80% instability (Figure 3). This proximity to MMRs could indicate possible main-belt origins. Moreover, JFCs' arguments of perihelia tend to concentrate near 0° and 180° (Quinn et al. 1990), and there is no such correlation for the sporadic JFC-like fireballs in this study (see supplementary material). This further supports a dominantly main-belt, asteroidal source.

Based on the calculated PE values, most of the events are also very durable and classified as type I chondritic material. In

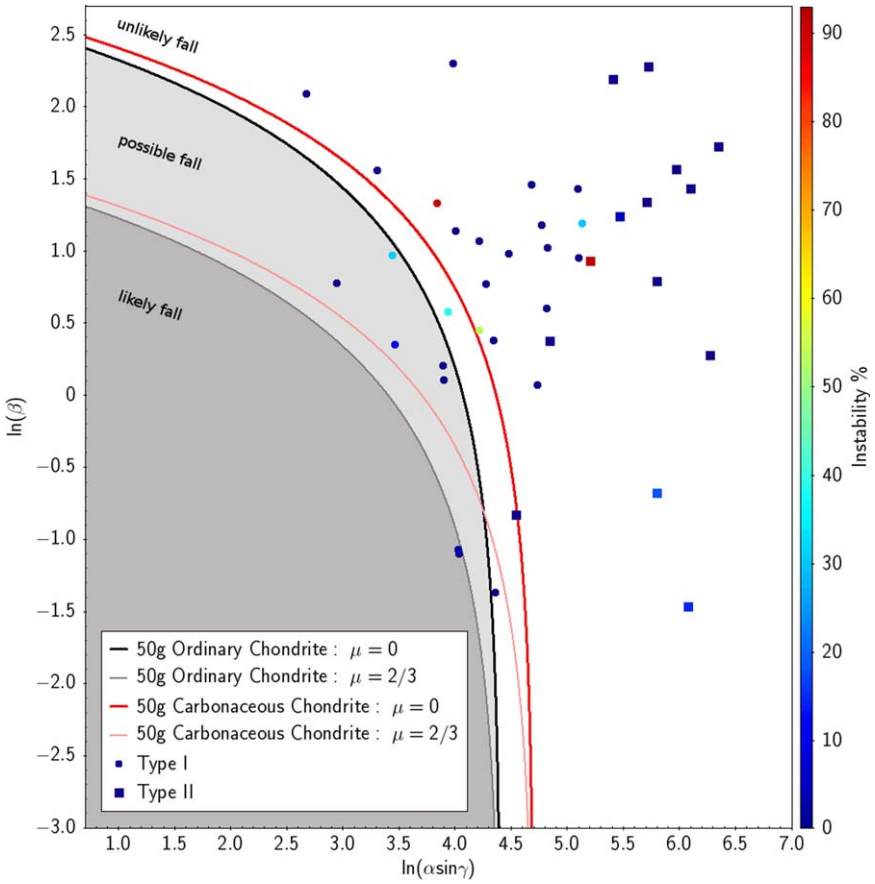

Figure 4. Distribution of nonshower JFC fireballs with enough deceleration to determine α–β values (at least ~20% deceleration). Here γ is the trajectory slope relative to the horizontal. If a macroscopic event is considered to have a final mass of $\geqslant$50 g, assuming $\rho_m = [2240, 3500]$ kg m^{-3} (carbonaceous and ordinary chondrite, respectively) and $c_{dA} = 1.5$, meteorite-dropping events can easily be identified given the range of possible shape change coefficients (μ).

fact, all of the fireballs in this sample are classified as either chondritic or carbonaceous chondritic material (type I or II; Figure 3). No events have PE types traditionally associated with cometary material (type III). However, it has been previously argued that primitive carbonaceous chondrites may have come from cometary sources (Gounelle et al. 2008). Thus, any DFN events that likely evolved chaotically over the previous 10 kyr (>50%) and are of type II were also considered cometary. At most, only two of the meteoroids studied here are likely to originate from a short-period comet (DN150817_01 and DN161028_02). However, this would require centimeter-to-meter cometary debris to be stronger than expected. The subset of weaker type II meteoroids in our data is also generally smaller (<50 g), perhaps debris released by dark carbonaceous asteroids in the outer main belt (DeMeo & Carry 2014; DeMeo et al. 2015; Takir et al. 2015). A novel process has been recently observed to release centimeter-sized particles on carbonaceous asteroid Bennu during the OSIRIS-REx mission (Lauretta et al. 2019).

However, caution should be used with such a criterion to characterize meteoroids; a wide range of meteorite types have been recovered from type II/III events. For example, Almahatta Sitta (2008 TC3), Košice, and Sutter's Mill had PE values near the II/IIIa boundary, despite all being of different meteorite types on asteroidal orbits (polymict breccia, H5, and CM2, respectively; Borovička et al. 2015; Brown et al. 2016). This is indicative that other physical factors, such as macroscopic cracks or porosity, can significantly affect the apparent strengths of impactors, and that there is still much unknown about the physical nature of meter-scale NEOs (Borovička et al. 2017, 2020). The PE criterion is useful to characterize the relative strength of meteoroids, but how much the meteorite type influences the strength is debatable.

4.1. Meteoroids Beyond the 2:1 Resonance

Previous studies have shown that a minor component of main-belt material can be transferred to JFC-like orbits and, in some circumstances, even onto dynamically unstable orbits via close encounters with the terrestrial planets (Fernández et al. 2002, 2014; Hsieh & Haghighipour 2016; Shober et al. 2020a, 2020b). Nevertheless, these objects' semimajor axes are predicted to be primarily constrained to the original range of the main belt (Hsieh & Haghighipour 2016). Here we see that of the four events beyond 3.27 au, two are likely asteroidal in origin based on their PE classifications and stability (Figure 3). The two most probable events to originate from unstable comet-like orbits are DN150817_01 and DN161028_02, with $86.1\% \pm 5.5\%$ and $90.8\% \pm 3.0\%$ probabilities of having chaotic histories based on Monte Carlo simulations along with orbits beyond the 2:1 MMR (each around $a \sim 3.6$ au). The meteoroids from events DN150817_01 and DN161028_02 both fall into type II, nominally carbonaceous and equally as or more durable than much of the main-belt debris (Figure 3). Even if both events are genuinely cometary in origin, they only comprise 4% of the sample.

4.2. Statistical Significance

Let us consider the null hypothesis to be that the source regions of sporadic meteoroids on JFC orbits match those of kilometer-scale JFCs. A P-test was used to determine if our results were significant enough to reject the null hypothesis. The *P*-value reflects the probability of observing a result at least as extreme as the one measured. We considered a *P*-value of 0.01 to be significant enough to reject the null hypothesis. At most, two events are genetically cometary within the data set (DN150817_01 and DN161028_02). Both of these events meet the criteria of being relatively weaker (type II) and likely originating from unstable orbits over the previous 10 kyr (>50%). We assume that the probability of observing a meteoroid from the main belt within our sample matches the maximum value found from a dynamical study based on telescopic observations (19 out of 58 JFCs from the main belt; Fernández & Sosa 2015). From these results, we find the *P*-value to be equal to 3.1×10^{-21}. This extraordinarily low probability clearly indicates that we can reject the null hypothesis. Thus, the source region for centimeter-scale meteoroids on JFC-like orbits does not match the cometary kilometer-sized bodies.

We additionally utilized Bayesian inference to estimate the proportion of main-belt material on JFC-like orbits (Salvatier et al. 2016). The informed prior used is a beta distribution with hyperparameters $\alpha = [1.38, 8.62]$ and an observation vector $c = [48, 2]$. The hyperparameters are derived from observational data, but the weight of these prior observations on our expected values was slightly reduced, as they corresponded to kilometer-scale objects (Fernández & Sosa 2015). Using a Markov Chain Monte Carlo to draw samples from the posterior distribution, we found that sporadic JFC-like meteoroids in NEO space are $82.1\% \pm 4.9\%$ from the main belt and $17.9\% \pm 4.9\%$ from the trans-Neptunian region with our reasonably informed prior. When an uninformed prior is used (i.e., the prior probability of observing a JFC or main-belt meteoroid is equal), the relative components are $94.2\% \pm 3.2\%$ from the main belt and $5.8\% \pm 3.2\%$ from JFCs.

Furthermore, while processing the data in this study, we found that of the meteoroids originating from JFC-like orbits with initial masses greater than 10 g, about $78\% \pm 3\%$ were sporadic and $22\% \pm 3\%$ were associated with showers. Thus, even when considering showers along with the sporadic population, it is likely that main-belt material makes up the majority of near-Earth material on orbits with $2 < T_J < 3$ within this size range. Evidently, the Tisserand's parameter is not a very informative metric when analyzing meteoroids in the inner solar system.

4.3. Why Are There No Sporadic Cometary Meteoroids?

4.3.1. Alternative Explanations

A possible explanation for the lack of dynamically unstable meteoroids in our sample could be that nongravitational forces are decoupling the material from Jupiter. Previous work has found that sporadic micron-sized meteoroids of the zodiacal cloud are not able to decouple from Jupiter via planetary perturbations along with solar radiation pressure before having another close encounter removing them from Earth-crossing orbits (Nesvorný et al. 2010). However, the meteoroids studied by Nesvorný et al. (2010) are in a completely different size range compared to those discussed here, and the effects on these meteoroids are very different.

Nevertheless, nongravitational forces are highly unlikely to be responsible for the meteoroids with asteroidal dynamics in our data set. Nongravitational forces, such as the Yarkovsky effect, would not be efficient enough to decouple these meteoroids before having another close encounter with Jupiter ($<10^3$ yr).

Alternatively, one could argue that we may not expect to see many JFC meteoroids on these low-perihelion orbits or within the examined size range (10 g to a few kilograms). First, there have been multiple studies of Earth-crossing JFCs, with the current number known to be ~140 objects (http://ssd.jpl.nasa.gov/horizons.cgi). A previous study investigated the dynamic stability of 58 JFCs in orbits with $q < 1.3$ au, and they found that most of the objects (over two-thirds) move on unstable orbits over ±10 kyr (Fernández & Sosa 2015). Thus, showing at the kilometer scale, objects on these orbits are dominated by weak genetically cometary material. Second, larger meteoroids (centimeter or larger) are capable of being produced by comets through a few mechanisms, such as cometary splitting or gas drag (Boehnhardt 2004; Fernández 2009). Thus, we should expect to observe cometary meteoroids within the range detected by the DFN.

4.3.2. Short Physical Lifetimes

Given the numerous JFCs on Earth-crossing orbits and their ability to produce meteoroids within the range considered in this study, it is surprising that we observe almost no meteoroids clearly sourced from the JFC population (Fernández & Morbidelli 2006). According to debiased NEO models, as much as 10% of the NEO population at the smallest sizes considered (~100 m) should be sourced from the JFC population (Granvik et al. 2018). Yet in this sample, we see no distinctly cometary meteoroids.

This lack of cometary debris within the sporadic population strongly supports the hypothesis that subkilometer JFCs have limited physical lifetimes in the inner solar system (Fernández et al. 2002; Meech et al. 2004; Fernández & Morbidelli 2006; Nesvorný et al. 2017). The physical lifetimes of centimeter–meter debris must be less than ~1000 yr (the decoherence time). This physical breakdown is consistent with the observations that there are less highly volatile asteroids at low perihelion distances (Granvik et al. 2016). Planetary debris seems to break down in the inner solar system closer to the Sun, depending on the object's size and volatile content. At large sizes ($>10^{3-4}$ m), material from the trans-Neptunian region is dominant on JFC-like orbits. However, as the diameters decrease to typical meteorite-producing objects, the physical lifetimes are likely so short that main-belt material becomes a more viable source. Conversely, according to Nesvorný et al. (2010), micron-sized meteoroid impacts on Earth are dominated by JFC particles (~85% of the mass influx). If accurate, these results suggest that dust- and kilometer-sized objects on JFC-like orbits are genetically cometary; however, intermediate sizes are sourced from the main asteroid belt. This is consistent with the prediction by Nesvorný et al. (2010) that centimeter-sized particles ejected from comets likely quickly disrupt (<10 kyr) and form the robust micron-sized population observed within the zodiacal cloud.

4.4. Meteorites from JFCs

A couple of the fireballs likely resulted in surviving meteorites >50 g (Figure 4); however, all of these are dynamically stable over the previous 10 kyr and only have PE values of type I. Thus, even on the occasion where we do have some genetically cometary material impact the Earth, according to our sample, it is unlikely to survive. It has been argued that primitive carbonaceous chondrites may be the best candidates to originate from cometary bodies; however, given our results, this may be only possible if the meteoroid was recently released from the parent body (within 1000 yr; Gounelle et al. 2008). While the cosmic-ray exposure ages are significantly shorter for some carbonaceous chondrites (<1 Myr), they are still usually much longer than the $\sim 10^3$ yr expected from our results (Eugster et al. 2006). Therefore, meteorites from $2 < T_J < 3$ orbits are expected, but they will not be cometary.

4.5. Limitations

This study is constrained by the amount of data collected by the DFN. However, given that the DFN is the largest fireball network in the world, this cannot be improved upon. Additionally, the PE value methodology is a very limited metric of meteoroid strength, as macroscopic features of the meteoroids can significantly affect the strengths. However, the PE value was utilized liberally in this study to determine potentially cometary meteoroids. Any meteoroid with a slightly weaker strength was considered as potentially cometary. Even with this very inclusive criterion, we found almost no meteoroids that fulfilled our physical and orbital requirements to be considered cometary. The results clearly demonstrate that cometary debris larger than dust-sized is too friable to survive in near-Earth space for longer periods.

5. Summary

Sporadic fireball data collected by the DFN demonstrates that there is a lack of cometary material on JFC-like orbits for meteoroids in the gram-to-kilogram size range. This supports the short physical lifetime hypothesis for JFC material (Fernández et al. 2002; Meech et al. 2004; Fernández & Morbidelli 2006; Nesvorný et al. 2017). Additionally, it indicates that the primary source region for Earth-crossing material on JFC-like orbits ($2 < T_J < 3$) is size-dependent. A majority of the objects at dust sizes and on kilometer scales are likely sourced from the trans-Neptunian region of the outer solar system (Nesvorný et al. 2010; Fernández & Sosa 2015). However, objects centimeters to meters in size are dominated by asteroidal material diffused out from the main belt. This diffusion process likely occurs via some combination of orbital resonances, Kozai resonances, nongravitational forces, and close encounters with terrestrial planets (Bottke et al. 2002; Fernández et al. 2014; Hsieh & Haghighipour 2016; Shober et al. 2020a, 2020b). In this study, we found a minor fraction of unstable, possibly cometary objects, but the number of fireballs observed to originate from stable orbits from the main belt over the previous 10 kyr is statistically significant. We estimate that as much as $94.2\% \pm 3.2\%$ of Earth-crossing centimeter-sized debris on these orbits is sourced from the main belt. Furthermore, considering that $22\% \pm 3\%$ of the JFC-like fireballs observed by the DFN over the previous 5 yr are associated with showers, our results suggest that the majority of centimeter material on JFC-like orbits in near-Earth space is main belt in origin. Thus, we should expect to see ordinary types of meteorite falls coming from Jupiter-crossing orbits.

This work was funded by the Australian Research Council as part of the Australian Discovery Project scheme (DP170102529). The SSTC authors acknowledge institutional support from Curtin University. This work was also supported by resources provided by the Pawsey Supercomputing Centre with funding from the Australian Government and the Government of Western Australia. This research made use of TOPCAT for visualization and figures (Taylor 2005). This research also made use of Astropy, a community-developed core Python package for astronomy (Robitaille et al. 2013). Simulations in this paper made use of the REBOUND code, which can be downloaded freely at http://github.com/hannorein/REBOUND (Rein & Liu 2012). The authors declare no competing interests. All data needed to evaluate the conclusions in the paper are present in the paper and/or at https://doi.org/10.5281/zenodo.4710556.

ORCID iDs

P. M. Shober https://orcid.org/0000-0003-4766-2098
E. K. Sansom https://orcid.org/0000-0003-2702-673X
H. A. R. Devillepoix https://orcid.org/0000-0001-9226-1870
M. C. Towner https://orcid.org/0000-0002-8240-4150

References

A'Hearn, M. F., Belton, M., Delamere, W., et al. 2005, Sci, 310, 258
Asher, D., Clube, S., & Steel, D. 1993, MNRAS, 264, 93
Boehnhardt, H. 2004, in Comets II, ed. M. C. Festou, H. U. Keller, & H. A. Weaver (Tucson, AZ: Univ. Arizona Press), 301
Borovička, J., Popova, O., & Spurný, P. 2019, M&PS, 54, 1024
Borovička, J., Spurný, P., & Brown, P. 2015, Asteroids IV, Vol. 257
Borovička, J., Spurný, P., Grigore, V. I., & Svoreň, J. 2017, P&SS, 143, 147
Borovička, J., Spurný, P., & Koten, P. 2007, A&A, 473, 661
Borovička, J., Spurný, P., & Shrbený, L. 2020, AJ, 160, 42
Borovička, J., Tóth, J., Igaz, A., et al. 2013, M&PS, 48, 1757
Bottke, W. F., Jr., Morbidelli, A., Jedicke, R., et al. 2002, Icar, 156, 399
Brown, P., Marchenko, V., Moser, D. E., Weryk, R., & Cooke, W. 2013, M&PS, 48, 270
Brown, P., Wiegert, P., Clark, D., & Tagliaferri, E. 2016, Icar, 266, 96
Brown, P. G., Hildebrand, A. R., Zolensky, M. E., et al. 2000, Sci, 290, 320
Brownlee, D. E., Horz, F., Newburn, R. L., et al. 2004, Sci, 304, 1764
Ceplecha, Z. 1994, A&A, 286, 967
Ceplecha, Z., Borovička, J., Elford, W. G., et al. 1998, SSRv, 84, 327
Ceplecha, Z., & McCrosky, R. 1976, JGR, 81, 6257
Consolmagno, G., Britt, D., & Macke, R. 2008, Geoch, 68, 1
DeMeo, F., Alexander, C., Walsh, K., Chapman, C., & Binzel, R. 2015, in Asteroids IV, ed. P. Michel, F. E. DeMeo, & W. F. Bottke (Tucson, AZ: Univ. Arizona Press), 13
DeMeo, F. E., & Carry, B. 2014, Natur, 505, 629
Devillepoix, H. A., Bland, P. A., Sansom, E. K., et al. 2019, MNRAS, 483, 5166
Devillepoix, H. A. R., Cupák, M., Bland, P. A., et al. 2020, P&SS, 191, 105036
Di Sisto, R. P., Fernández, J. A., & Brunini, A. 2009, Icar, 203, 140
Drummond, J. D. 1981, Icar, 45, 545
Duncan, M., Levison, H., & Dones, L. 2004, Comets II (Tucson, AZ: Univ. Arizona Press), 193
Duncan, M. J., & Levison, H. F. 1997, Sci, 276, 1670
Eugster, O., Herzog, G., Marti, K., & Caffee, M. 2006, in Meteorites and the Early Solar System II, ed. D. S. Lauretta & H. Y. McSween, Jr. (Tucson, AZ: Univ. Arizona Press), 829
Fernández, J. A., Gallardo, T., & Brunini, A. 2002, Icar, 159, 358
Fernández, J. A., & Morbidelli, A. 2006, Icar, 185, 211
Fernández, J. A., & Sosa, A. 2015, P&SS, 118, 14

Fernández, J. A., Sosa, A., Gallardo, T., & Gutiérrez, J. N. 2014, Icar, 238, 1
Fernández, Y., Kelley, M., Lamy, P., et al. 2013, Icar, 226, 1138
Fernández, Y. R. 2009, P&SS, 57, 1218
Fernández, Y. R., Jewitt, D. C., & Sheppard, S. S. 2005, AJ, 130, 308
Fornasier, S., Hasselmann, P., Barucci, M., et al. 2015, A&A, 583, A30
Gounelle, M., Morbidelli, A., Bland, P. A., et al. 2008, in The Solar System Beyond Neptune, ed. M. A. Barucci, D. P. Cruikshank, & A. Morbidelli (Tucson, AZ: Univ. Arizona Press), 525
Granvik, M., & Brown, P. 2018, Icar, 311, 271
Granvik, M., Morbidelli, A., Jedicke, R., et al. 2016, Natur, 530, 303
Granvik, M., Morbidelli, A., Jedicke, R., et al. 2018, Icar, 312, 181
Gritsevich, M., & Stulov, V. 2006, SoSyR, 40, 477
Gritsevich, M. I. 2007, SoSyR, 41, 509
Howie, R. M., Paxman, J., Bland, P. A., et al. 2017, ExA, 43, 237
Hsieh, H. H., & Haghighipour, N. 2016, Icar, 277, 19
Jansen-Sturgeon, T., Sansom, E. K., & Bland, P. A. 2019, M&PS, 54, 2149
Jenniskens, P. 2006, Meteor Showers and Their Parent Comets (Cambridge: Cambridge Univ. Press)
Jopek, T. J. 1993, Icar, 106, 603
Lauretta, D., Hergenrother, C., Chesley, S., et al. 2019, Sci, 366, 6470
Levison, H. F., & Duncan, M. J. 1994, Icar, 108, 18
Levison, H. F., & Duncan, M. J. 1997, Icar, 127, 13
Lyytinen, E., & Gritsevich, M. 2016, P&SS, 120, 35
Madiedo, J. M., Trigo-Rodríguez, J. M., Zamorano, J., et al. 2014, A&A, 569, A104
Meech, K., Hainaut, O., & Marsden, B. 2004, Icar, 170, 463
Nesvorný, D., Jenniskens, P., Levison, H. F., et al. 2010, ApJ, 713, 816
Nesvorný, D., Vokrouhlický, D., Dones, L., et al. 2017, ApJ, 845, 27
Popova, O., Borovička, J., Hartmann, W. K., et al. 2011, M&PS, 46, 1525
Quinn, T., Tremaine, S., & Duncan, M. 1990, ApJ, 355, 667
Rein, H., & Liu, S. F. 2012, A&A, 537, A128
Rein, H., & Spiegel, D. S. 2015, MNRAS, 446, 1424
Robitaille, T. P., Tollerud, E. J., Greenfield, P., et al. 2013, A&A, 558, A33
Salvatier, J., Wiecki, T. V., & Fonnesbeck, C. 2016, PeerJ Computer Science, 2, e55
Sansom, E. K., Bland, P., Paxman, J., & Towner, M. 2015, M&PS, 50, 1423
Sansom, E. K., Gritsevich, M., Devillepoix, H. A., et al. 2019a, ApJ, 885, 115
Sansom, E. K., Jansen-Sturgeon, T., Rutten, M. G., et al. 2019b, Icar, 321, 388
Shober, P. M., Jansen-Sturgeon, T., Bland, P., et al. 2020a, MNRAS, 498, 5240
Shober, P. M., Jansen-Sturgeon, T., Sansom, E. K., et al. 2020b, AJ, 159, 191
Southworth, R., & Hawkins, G. 1963, SCoA, 7, 261
Spurný, P., Borovička, J., Baumgarten, G., et al. 2017, P&SS, 143, 192
Sunshine, J., A'hearn, M., Groussin, O., et al. 2006, Sci, 311, 1453
Takir, D., Emery, J. P., & McSween, H. Y., Jr. 2015, Icar, 257, 185
Tancredi, G. 1995, A&A, 299, 288
Tancredi, G. 2014, Icar, 234, 66
Taylor, M. B. 2005, adass XIV, 347, 29
Towner, M. C., Cupák, M., Deshayes, J., et al. 2020, PASA, 37, e008
Wetherill, G., & ReVelle, D. 1981, Icar, 48, 308